

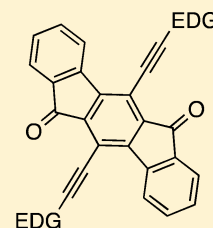
Synthesis and Optoelectronic Properties of Indeno[1,2-*b*]fluorene-6,12-dione Donor–Acceptor–Donor Triads

Conerd K. Frederickson and Michael M. Haley*

Department of Chemistry & Biochemistry and Materials Science Institute, University of Oregon, Eugene, Oregon 97403-1253, United States

Supporting Information

ABSTRACT: We report the synthesis of donor–acceptor–donor triads based on the indeno[1,2-*b*]fluorene-6,12-dione (IF) scaffold. Arylethynyl donor group attachment expands the light absorption of these molecules to the 600–700 nm region compared to derivatives with nondonating silylethynyl substituents yet does not affect the electron-accepting capabilities of the IF core. All triads show reduction potentials at similar or less negative potentials compared to the silylethynyl derivatives. Protonation studies using the bis(dibutylanilino) triad verify the charge transfer nature of the expanded absorption profile.



Intramolecular charge transfer (ICT) in polycyclic conjugated hydrocarbons is a phenomenon that has been widely employed for the synthesis of low band gap chromophores.¹ These compounds, consisting of electron donating (D) and electron accepting (A) components connected by a π -conjugated bridge, have been used in a vast array of organic electronic materials including field effect transistors,^{2–4} light emitting diodes,^{5,6} fluorescent sensors,⁷ nonlinear optics,⁸ and photovoltaics.⁹ The modular nature of donor–acceptor systems means they offer exceptional tunability by altering the paired donor and acceptor groups to produce the desired properties.

Our lab has been exploring new electron-accepting molecules based on the isomers of the pentacyclic indenofluorene (IF) scaffold.¹⁰ Indeno[1,2-*b*]fluorene derivatives (e.g., **1**, Figure 1) have attracted significant investigation due to their simple synthesis from commercially available starting materials (**2**) and their resemblance to linear acenes. Not only do OFET devices made from derivatives of **1** show ambipolar charge transport,^{11,12} but recent work also has shown that the precursor diones can act as n-type electronic materials. For example, compound **3** was used in the first field effect transistor manufactured using an IF-dione derivative, although the device only displayed a mobility of $2.93 \times 10^{-5} \text{ cm}^2 \text{ V}^{-1} \text{ s}^{-1}$.¹³ In 2008 the Yamashita group produced an OFET using dione **4** that achieved a much higher mobility of $0.17 \text{ cm}^2 \text{ V}^{-1} \text{ s}^{-1}$.¹⁴ The Park group in 2011 obtained a similar mobility ($0.16 \text{ cm}^2 \text{ V}^{-1} \text{ s}^{-1}$) for hexafluorinated derivative **5**.¹⁵

Following evidence that these more stable dione compounds could also be used as active materials in OFETs, our group expanded research into exploring their properties.^{13–15} Previous work examined the effect different silylethynyl substituents (e.g., **6**) had on the crystal packing.¹⁶ This study was limited initially by the fact that iodide precursor **7** was not stable in the presence of heat and light and its synthesis involved a shock-sensitive intermediate; thus, it could only be isolated in small quantities.¹⁷ To permit more extensive research into dione derivatives, our lab recently devised a

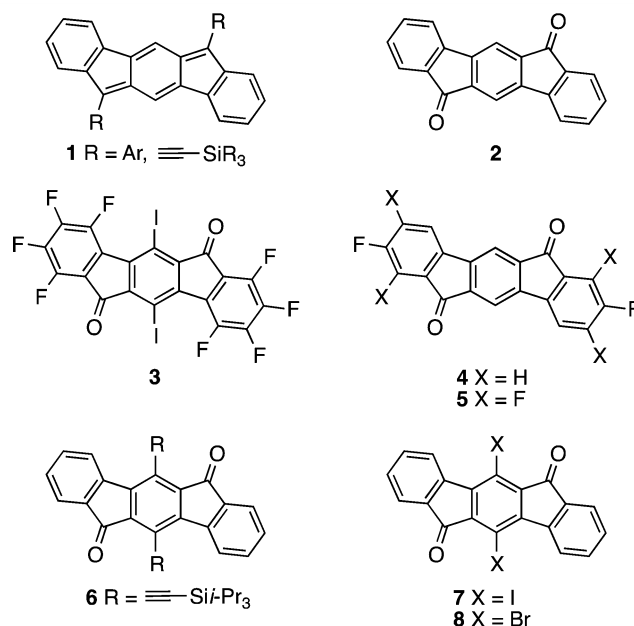


Figure 1. Indeno[1,2-*b*]fluorene-6,12-dione and derivatives.

synthetic route to multigram amounts of the dibrominated dione **8**,¹⁸ thereby opening the door to new, center-function-alized derivatives of **2**.

Herein we describe the synthesis of symmetric donor–acceptor–donor triads **9a–e** (Figure 2) based on the indeno[1,2-*b*]fluorene-6,12-dione scaffold. While there has been some research into D–A compounds including the [1,2-*b*]IF skeleton, previous studies utilized substitution on the outer phenyl rings,² and most compounds contained sp^3 carbon atoms at the apex of the five-membered rings and thus used the

Received: August 31, 2014

Published: October 20, 2014



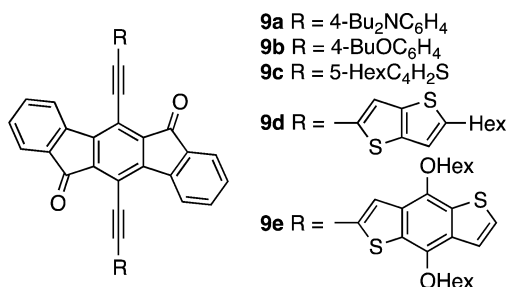
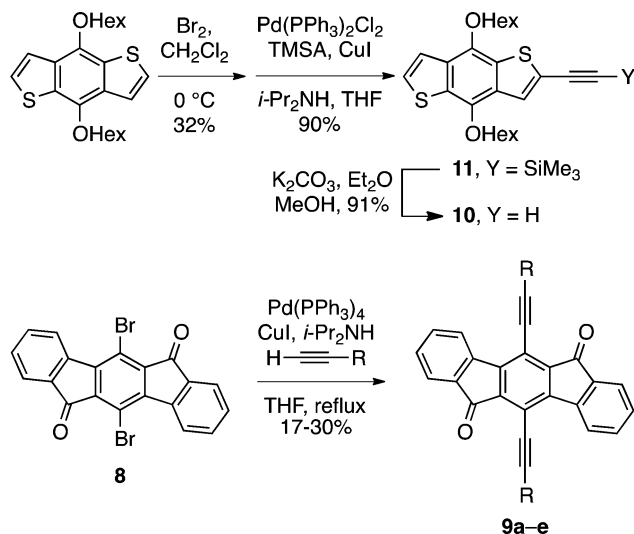


Figure 2. Target donor–acceptor–donor triads **9a–e**.

IF backbone as the π bridge instead of the acceptor.^{10,19,20} Compounds **9a–e** utilize ethynyl groups as the π bridge while simultaneously taking advantage of their inductive electron-withdrawing nature to retain the lowered LUMO level seen in the silylethynyl derivatives such as **6**.^{16,18} Variation of the donor group attached to the ethynyl linkers permits investigation into the effect of different strength donor groups while retaining the same acceptor moiety. The introduction of ITC to the dione core should allow the production of low band gap compounds that retain the electron accepting capabilities and low lying LUMO energy levels of the previously studied silylethynyl substituted molecules.

The donor-substituted terminal acetylenes for triads **9a–d** were prepared via literature procedures,²¹ whereas alkyne **10** required for **9e** was unknown and thus was assembled as shown in Scheme 1. Monobromination of 4,8-bis(hexyloxy)-

Scheme 1. Syntheses of Alkyne **10** and Triads **9a–e**



benzodithiophene²² with Br₂ followed by Sonogashira cross-coupling with (trimethylsilyl)acetylene gave **11** in modest yield. Subsequent deprotection with K₂CO₃ in MeOH furnished **10**, which was used immediately without purification. The final triads were synthesized by cross-coupling of the donor alkynes and dibromodione **8** to produce compounds **9a–e** as amorphous powders. The low isolated yields of the triads were attributable to significant material loss during purification, which involved trituration with hexanes followed by dissolution of the solid in CH₂Cl₂ and precipitation into MeOH.

The electronic absorption spectra of D–A–D triads **9a–e**, along with the spectrum of the nondonor TIPS-ethynyl derivative **6**, are shown in Figure 3. As can be seen, compounds

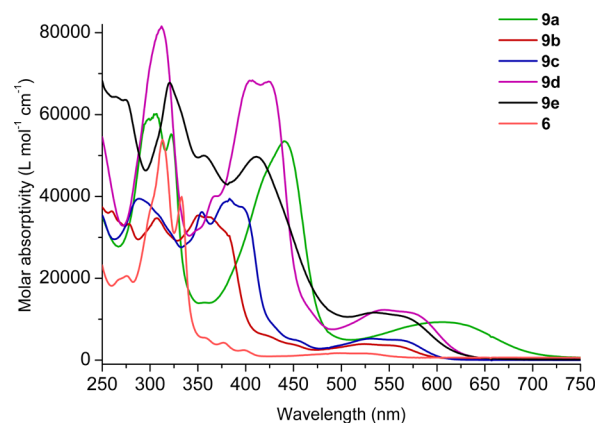


Figure 3. Electronic absorption spectra of triads **9a–e** and nondonor dione **6** in CHCl₃.

9a–e all exhibit higher molar absorptivity in the low energy region than **6**, which we attribute to charge transfer behavior. Compounds **9a** and **9d** show the largest red shift in absorption with their lowest energy peaks at 607 and 566 nm, respectively, compared to 525 nm for **6**. Both triads show a similar spectral shape with a large peak located near 450 nm and a broad low energy peak that extends past 600 nm, indicative of an ICT absorption.^{21a}

Further evidence of intramolecular charge transfer in the excited state of these molecules can be seen from their fluorescence spectra (Figure 4). Compounds **9b** and **9c** both demonstrate solvatochromic behavior in their fluorescence spectra. The emission maxima for both compounds exhibit a significant bathochromic shift, with the emission maxima shifting from 561 and 559 nm in cyclohexane to 605 and 615 nm in DMSO, respectively. This is consistent with the higher

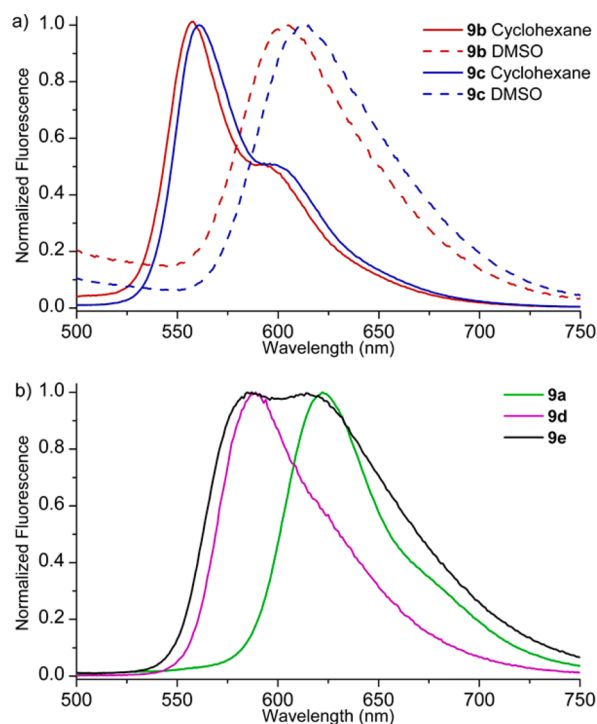


Figure 4. Fluorescence spectra of (a) **9b** and **9c** in cyclohexane and DMSO, and (b) **9a**, **9d**, and **9e** in cyclohexane.

energy emission from the nonpolar, local excited state being more prevalent in a nonpolar solvent and the lower energy emission from the polar, intramolecular charge transfer state being more prevalent in polar solvent. Figure 4b shows the emission of compounds **9a** and **9d–e** in cyclohexane. Due to the more strongly donating nature of the aryl groups on these compounds, these molecules only show emission for the charge transfer state in cyclohexane and are fully quenched in DMSO.

To assess how the UV–vis spectrum changed upon removal of the charge transfer absorbance, protonation studies of **9a** were undertaken (Figure 5). As the concentration of trifluoro-

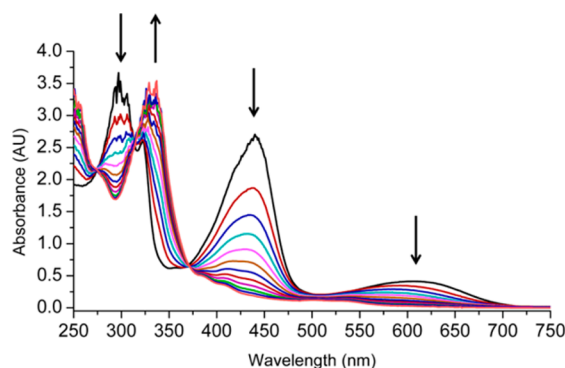


Figure 5. Change in UV–vis spectrum of **9a** upon the increase in TFA concentration.

acetic acid (TFA) is increased both low energy peaks at 441 and 607 nm decrease until they are no longer visible. The high energy peak at 305 nm also decreases and a new peak at 334 nm grows in its place. Addition of a large excess of TFA produces the red spectrum shown in Figure 6a. Comparison of this spectrum with the absorption profile for triisopropylsilyl

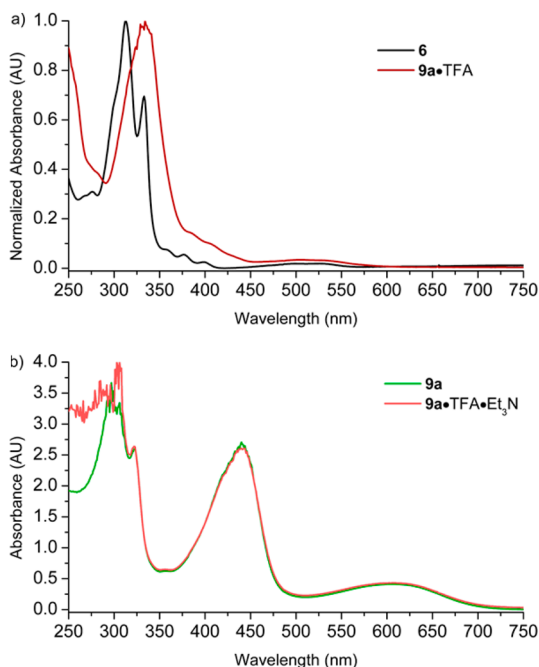


Figure 6. Comparison of the UV–vis spectra for (a) protonated **9a** (red) and triisopropylsilyl derivative **6** (black) and (b) **9a** before protonation (green) and after protonation/deprotonation with TFA/ Et_3N (orange).

derivative **6** (black) shows that, without the nitrogen lone pair available for charge transfer, the absorption spectrum is very similar to that of the nondonating derivative (Figure 6a). Finally, addition of excess Et_3N to fully protonated **9a** returns the original absorption spectrum (Figure 6b). This illustrates the reversibility of the process and is analogous to our earlier protonation studies of donor–acceptor-substituted phenylacetylene scaffolding.^{21a}

Cyclic voltammetry experiments were also performed on triads **9a–e** (Figure 7). All five molecules show two reversible

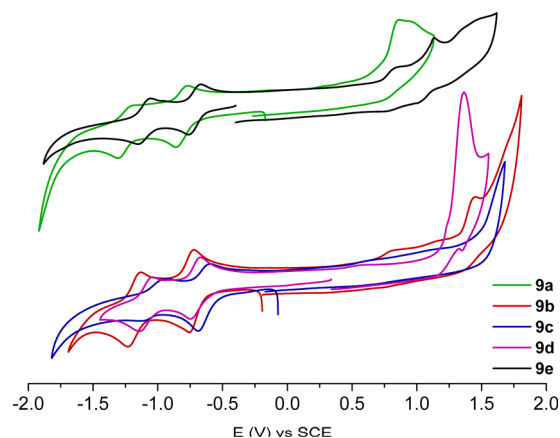


Figure 7. Cyclic voltammograms of triads **9a–e**.

reductions with the first reduction half wave potential between -0.64 and -0.82 V and the second between -1.09 to -1.24 V vs SCE (Table 1). The corresponding reduction potentials for **6** are -0.82 and -1.24 V, thus demonstrating that replacement of the silyl groups with donating aryl groups does not hinder the electron accepting capability of the indenofluorenedione core. While no reversible oxidations were present in any of the triads, most exhibit irreversible oxidations, with the peak anodic current of **9a**, **9d**, and **9e** in the 1.1 – 1.3 V range. The peak anodic current for oxidation of **9b** is at 1.64 V, whereas **9c** shows no oxidation(s) in the solvent window. Except for **9c**, the DAD triads reflect an increased ease of oxidation over the silyl ethynyl diones such as **6**, which did not show any oxidation peaks.¹⁶ These values are at a less positive potential than that of parent dione **2**, which has a reversible oxidation at 1.70 V.²²

In conclusion a series of donor–acceptor–donor triads based on the indeno[1,2-*b*]fluorene-6,12-dione core has been synthesized. The effects of the intramolecular charge transfer induction on their optical and electrochemical properties have been investigated. The triads retain the electron accepting character of the parent and other ethylated dione derivatives while extending the UV–vis absorption spectrum to lower energy. Currently the device applications of these compounds as well as DAD triads with fully conjugated indenofluorenes are being investigated.

EXPERIMENTAL SECTION

General. ^1H and ^{13}C NMR spectra were recorded in CDCl_3 using either a 300 MHz (^1H : 300.09 MHz) or 600 MHz (^1H : 600.02 MHz, ^{13}C : 150.89 MHz) spectrometer with a multinuclear broad-band cryoprobe. Chemical shifts (δ) are expressed in ppm relative to the residual CHCl_3 (^1H : 7.27 ppm, ^{13}C : 77.23 ppm). THF was distilled from a sodium benzophenone ketyl under nitrogen. Unless stated otherwise all solvents and reagents were used as received. Except for

Table 1. Electrochemical and Optical Data for Donor–Acceptor–Donor Triads 9a–e and Triisopropylsilyl Derivative 6

compd	Electrochemical ^a					Optical		
	E_{ox}^1 (V) ^b	$E_{\text{red}}^1, E_{\text{red}}^2$ (V) ^c	E_{HOMO} (eV) ^d	E_{LUMO} (eV) ^d	E_{gap} (eV)	λ_{abs} (nm)	E_{gap} (eV) ^e	λ_{em} (nm) ^f
9a	1.11	−0.82, −1.24	−5.75	−3.82	1.93	306, 322, 440, 608	2.04	636
9b	1.64	−0.76, −1.18	−6.24	−3.88	2.36	307, 351, 524, 548	2.26	561
9c	—	−0.64, −1.15	—	−4.00	—	289, 354, 383, 532, 554	2.24	559
9d	1.31	−0.71, −1.09	−5.95	−3.93	2.02	312, 404, 424, 546, 565	2.19	589
9e	1.27	−0.72, −1.10	−5.91	−3.93	1.98	274, 320, 356, 411, 534, 554	2.24	587
6 ^g	—	−0.82, −1.24	—	−3.82	—	313, 333, 500, 525	2.37	568

^aCVs were taken using 1–5 mM analyte in CH₂Cl₂ with 0.1 M Bu₄NBF₄ electrolyte and a scan rate of 50 mV s^{−1}. The working electrode was glassy carbon with a Pt wire counter and a Ag wire pseudoreference electrode. Values are presented vs SCE using the Fc/Fc⁺ couple (0.46 V) as an internal standard. ^bEstimated using the peak anodic current (E_p). ^cDetermined using the half wave potential. ^dApproximated using SCE = −4.64 eV vs vacuum and either $E_{1/2}$ values for reversible processes or E_p values for irreversible processes. ^eDetermined by using the maximum absorption of the lowest energy transition in the UV–vis spectrum. ^fSpectra taken in cyclohexane. ^gReference 16.

10, all other terminal donor arylacetylenes were prepared by literature methods.²¹

2-(Trimethylsilyl)ethynyl-4,8-bis(hexyloxy)benzo[1,2-*b*;3,4-*b'*]dithiophene (11). A solution of 4,8-bis(hexyloxy)benzo[1,2-*b*;3,4-*b'*]dithiophene²³ (1.4 g, 3.7 mmol) in CH₂Cl₂ (50 mL) was cooled to 0 °C, and then a solution of Br₂ (0.6 g, 3.7 mmol) in CH₂Cl₂ (50 mL) was added dropwise excluding light. After stirring overnight, the reaction was washed with H₂O (100 mL), satd NaHCO₃ solution (100 mL), and brine (100 mL). The organic layer was dried (MgSO₄), and the solvent was removed. The residue was purified by chromatography on silica gel (9:1 hexanes/CH₂Cl₂) to give the 2-bromobenzodithiophene (0.57 g, 32%) as a yellow oil. ¹H NMR (300 MHz, CDCl₃) δ 7.47 (s, 1H), 7.46 (d, J = 5.8 Hz, 1H), 7.40 (d, J = 5.8 Hz, 1H), 4.25 (pseudo q, J = 6.1 Hz, 4H), 1.93–1.85 (m, 4H), 1.63–1.55 (m, 4H), 1.45–1.37 (m, 8H), 0.99–0.94 (m, 6H); ¹³C NMR (600 MHz, CDCl₃) δ 143.6, 143.5, 131.6, 130.9, 130.65, 130.61, 126.3, 123.2, 120.3, 114.6, 74.1, 74.0, 31.6, 30.5, 25.7, 22.67, 22.65, 14.1.

A mixture of the 2-bromobenzodithiophene (0.57 g, 1.2 mmol), PdCl₂(PPh₃)₂ (42 mg, 0.06 mmol), CuI (30 mg, 0.15 mmol), THF (20 mL), and *i*-Pr₃NH (2.5 mL) was sparged for 20 min with N₂. (Trimethylsilyl)acetylene (0.2 mL, 1.4 mmol) was added via syringe, and the sealed reaction was stirred overnight at room temperature. The solvent was removed *in vacuo*, and the residue redissolved in hexane. The mixture was passed through a silica gel plug (hexanes) to give the (trimethylsilyl)ethynylbenzodithiophene (0.54 g, 90%) as a bright yellow oil. ¹H NMR (300 MHz, CDCl₃) δ 7.61 (s, 1H), 7.46 (d, J = 5.5 Hz, 1H), 7.38 (d, J = 5.6 Hz, 1H), 4.29 (t, J = 6.4 Hz, 2H), 4.27 (t, J = 6.4 Hz, 2H), 1.93–1.85 (m, 4H), 1.63–1.55 (m, 4H), 1.45–1.37 (m, 8H), 0.99–0.94 (m, 6H), 0.33 (s, 9H); ¹³C NMR (600 MHz, CDCl₃) δ 144.6, 143.8, 132.8, 130.7, 130.5, 129.9, 126.6, 126.1, 122.3, 120.3, 101.2, 98.0, 74.2, 73.9, 31.7, 30.5, 25.74, 25.71, 22.66, 22.65, 14.1, −0.2; HRMS (TOF-ESI) for C₂₇H₃₈O₂S₂Si [M⁺ + H]⁺: calcd 487.2161, found 487.2183.

2-Ethynyl-4,8-bis(hexyloxy)benzo[1,2-*b*;3,4-*b'*]dithiophene (10). To a solution of the ethynylsilane 11 (0.293 g, 0.6 mmol) in MeOH (10 mL) and Et₂O (10 mL) was added K₂CO₃ (0.465 g, 3.3 mmol), and the mixture stirred overnight. The mixture was diluted with hexane and washed with water. The organic layer was dried (MgSO₄), and the solvent was removed under vacuum to give the deprotected alkyne 10 (0.233 g, 91%) as an orange oil, which was used immediately in the next cross-coupling reaction. ¹H NMR (300 MHz, CDCl₃) δ 7.67 (s, 1H), 7.47 (d, J = 5.5 Hz, 1H), 7.39 (d, J = 5.5 Hz, 1H), 4.27 (t, J = 6.4 Hz, 2H), 4.25 (t, J = 6.4 Hz, 2H), 3.48 (s, 1H), 1.96–1.77 (m, 4H), 1.63–1.51 (m, 4H), 1.43–1.33 (m, 8H), 1.00–0.88 (m, 6H); ¹³C NMR (600 MHz, CDCl₃) δ 144.7, 143.9, 132.9, 130.50, 130.47, 129.9, 126.75, 126.73, 121.2, 120.3, 83.0, 77.5, 74.2, 74.0, 31.7, 30.5, 25.75, 25.72, 22.7, 14.1; HRMS (TOF-ESI) for C₂₄H₃₀O₂S₂ [M⁺+H]⁺: calcd 415.1765, found 415.1756.

General Procedure for D–A–D Triads Synthesis. To a dry 15 mL pressure tube under N₂ was added 5,11-dibrominden[1,2-*b*]fluorene-6,12-dione (8, 1 equiv), CuI (50 mol %), and Pd(PPh₃)₄ (10 mol %) before evacuating and backfilling twice with N₂. The

donor arylacetylene (2.5 equiv) in THF (6 mL) was added, and the reaction was sparged with N₂. After 1 h, *i*-Pr₃NH (1 mL) was added and the tube was sealed and heated overnight at 100 °C. After cooling to rt, the reaction mixture was diluted with CH₂Cl₂ and passed through a plug of silica gel (CH₂Cl₂). After the solvent was removed, the residue was triturated in hexanes and filtered followed by dissolution in CH₂Cl₂ and precipitation into MeOH three times.

Compound 9a. Dark blue-green solid, 23% yield. ¹H NMR (600 MHz, CDCl₃) δ 8.61 (d, J = 7.5 Hz, 2H), 7.71 (d, J = 7.3 Hz, 2H), 7.65 (d, J = 8.3 Hz, 4H), 7.57 (t, J = 7.5 Hz, 2H), 7.36 (t, J = 7.4 Hz, 2H), 6.68 (d, J = 8.2 Hz, 4H), 3.35 (t, J = 7.7 Hz, 8H), 1.63 (p, J = 7.2 Hz, 8H), 1.40 (s, J = 7.4 Hz, 8H), 1.00 (t, J = 7.4 Hz, 12H); ¹³C NMR (600 MHz, CDCl₃) δ 191.5, 149.0, 145.7, 142.8, 137.2, 134.8, 134.3, 133.8, 129.4, 123.9, 123.4, 114.6, 111.6, 108.3, 104.4, 84.1, 51.0, 29.6, 20.5, 14.2; UV–vis (CHCl₃) λ_{max} (ε) 306 (60 100), 322 (55 200), 440 (53 500), 608 (9260) nm; HRMS (TOF-ESI) for C₅₂H₅₂N₂O₂ [M⁺ + H]⁺: calcd 737.4107, found 737.4110.

Compound 9b. Bright red solid, 30% yield. ¹H NMR (600 MHz, CDCl₃) δ 8.54 (d, J = 7.5 Hz, 2H), 7.74 (d, J = 8.5 Hz, 4H), 7.71 (d, J = 7.3 Hz, 2H), 7.58 (t, J = 6.7 Hz, 2H), 7.38 (t, J = 7.4 Hz, 2H), 6.98 (d, J = 8.6 Hz, 4H), 4.06 (t, J = 6.5 Hz, 4H), 1.83 (d, J = 7.7 Hz, 4H), 1.56 (d, J = 7.6 Hz, 4H), 1.03 (t, J = 7.4 Hz, 6H); ¹³C NMR (600 MHz, CDCl₃) δ 191.0, 160.3, 145.9, 142.4, 137.6, 134.9, 134.0, 133.7, 129.6, 124.0, 123.2, 114.9, 114.5, 114.3, 102.2, 83.7, 67.9, 31.2, 19.2, 13.9; UV–vis (CHCl₃) λ_{max} (ε) 307 (34 700), 351 (35 400), 524 (3920), 548 (3630) nm; HRMS (TOF-ESI) for C₄₄H₃₄O₄ [M⁺+H]⁺: calcd 627.2535, found 627.2554.

Compound 9c. Maroon solid, 22% yield. ¹H NMR (600 MHz, CDCl₃) δ 8.36 (d, J = 7.5 Hz, 2H), 7.65 (d, J = 7.2 Hz, 2H), 7.53 (t, J = 7.5 Hz, 2H), 7.35 (d, J = 3.6 Hz, 2H), 7.33 (t, J = 7.5 Hz, 2H), 6.78 (d, J = 3.3 Hz, 2H), 2.87 (t, J = 7.6 Hz, 4H), 1.74 (p, J = 7.6 Hz, 4H), 1.47–1.41 (m, 4H), 1.39–1.34 (m, 8H), 0.93 (t, J = 7.0 Hz, 6H); ¹³C NMR (600 MHz, CDCl₃) δ 190.8, 151.2, 145.8, 142.3, 137.3, 135.0, 134.1, 133.9, 129.8, 125.0, 124.2, 123.4, 120.0, 113.9, 96.3, 88.6, 31.78, 31.76, 30.7, 29.0, 22.8, 14.3; UV–vis (CHCl₃) λ_{max} (ε) 289 (39 400), 354 (36 200), 383 (39 500), 532 (5250), 554 (4950) nm; HRMS (TOF-ESI) for C₄₄H₃₈O₂S₂ [M⁺ + H]⁺: calcd 663.2391, found 663.2394.

Compound 9d. Purple solid, 18% yield. ¹H NMR (600 MHz, CDCl₃) δ 8.30 (d, J = 7.3 Hz, 2H), 7.59 (d, J = 7.2 Hz, 2H), 7.55 (s, 2H), 7.50 (t, J = 7.4 Hz, 2H), 7.30 (t, J = 7.3 Hz, 2H), 6.93 (s, 2H), 3.73 (q, J = 7.6 Hz, 4H), 2.92 (t, J = 7.6 Hz, 4H), 1.76 (p, J = 8.0 Hz, 4H), 1.48–1.42 (m, 4H), 1.40–1.34 (m, 4H), 0.93 (t, J = 6.2 Hz, 6H); ¹³C NMR (600 MHz, CDCl₃) δ 190.5, 152.4, 145.7, 142.1, 141.8, 137.2, 134.0, 129.8, 126.1, 124.1, 123.3, 122.0, 116.6, 113.5, 96.7, 90.0, 58.7, 31.8, 31.65, 31.61, 29.1, 22.8, 18.7, 14.3; UV–vis (CHCl₃) λ_{max} (ε) 312 (81 600), 404 (68 300), 424 (68 100), 546 (12 200), 565 (11 800) nm; HRMS (TOF-ESI) for C₄₈H₃₈O₂S₄Na [M⁺ + Na]⁺: calcd 797.1652, found 797.1645.

Compound 9e. Green solid, 17% yield. ¹H NMR (600 MHz, CDCl₃) δ 8.43 (d, J = 7.5 Hz, 2H), 7.86 (s, 2H), 7.71 (d, J = 7.3 Hz, 2H), 7.63 (t, J = 7.4 Hz, 2H), 7.40 (d, J = 5.4 Hz, 2H), 7.37–7.33 (m,

4H), 4.32 (t, $J = 6.5$ Hz, 4H), 4.26 (t, $J = 6.5$ Hz, 4H), 1.94–1.84 (m, 8H), 1.65–1.56 (m, 8H), 1.48–1.40 (m, 16H), 0.98 (m, 12H); ^{13}C NMR (600 MHz, CDCl_3) δ 190.3, 145.9, 145.0, 143.8, 142.0, 137.3, 135.0, 133.9, 133.1, 130.7, 130.6, 130.4, 129.8, 127.3, 124.1, 123.3, 121.6, 120.4, 113.2, 95.8, 90.4, 31.7, 30.5, 29.7, 25.81, 25.78, 22.7, 14.2; UV-vis (CHCl_3) λ_{max} (ϵ) 274 (63 600), 320 (67 800), 356 (50 000), 411 (49 700), 534 (11 600), 554 (11 100) nm; HRMS (TOF-ESI) for $\text{C}_{62}\text{H}_{55}\text{O}_6\text{S}_4$ [$\text{M}^+ - \text{C}_6\text{H}_{13} + 2\text{H}$]: calcd 1023.2882, found 1023.2881.

■ ASSOCIATED CONTENT

■ Supporting Information

Spectroscopic data for all new compounds can be found in the Supporting Information. This material is available free of charge via the Internet at <http://pubs.acs.org>.

■ AUTHOR INFORMATION

Corresponding Author

*E-mail: haley@uoregon.edu.

Notes

The authors declare no competing financial interest.

■ ACKNOWLEDGMENTS

We thank the National Science Foundation (CHE-1301485) for support of this research. We would also like to thank Prof. Shannon Boettcher for use of one of his group's potentiostats. HRMS data were obtained at the Mass Spectrometry Facilities and Services Core of the Environmental Health Sciences Center, Oregon State University, supported by Grant No. P30-ES00210, National Institute of Environmental Health Sciences, National Institutes of Health.

■ REFERENCES

- (1) Ajayaghosh, A. *Chem. Soc. Rev.* **2003**, *32*, 181–191.
- (2) Usta, H.; Risko, C.; Wang, Z.; Huang, H.; Deliomeroglu, M. K.; Zhukhovitskiy, A.; Facchetti, A.; Marks, T. J. *J. Am. Chem. Soc.* **2009**, *131*, 5586–5608.
- (3) Huang, W.; Yang, B.; Sun, J.; Liu, B.; Yang, J.; Zou, Y.; Xiong, J.; Zhou, C.; Gao, Y. *Org. Electron.* **2014**, *15*, 1050–1055.
- (4) Yu, A.-D.; Kurosawa, T.; Ueda, M.; Chen, W.-C. *J. Polym. Sci., Part A: Polym. Chem.* **2014**, *52*, 139–147.
- (5) Yoon, J.; Lee, J. S.; Yoon, S. S.; Kim, Y. K. *Bull. Korean Chem. Soc.* **2014**, *35*, 1670–1674.
- (6) Reckefuss, N.; Rojahn, M.; Mu, C. D.; Rudati, P.; Frohne, H.; Nuyken, O.; Becker, H.; Meerholz, K. *Nature* **2003**, *42*, 829–833.
- (7) Thomas, S. W.; Joly, G. D.; Swager, T. M. *Chem. Rev.* **2007**, *107*, 1339–1386.
- (8) Si, P.; Liu, J.; Deng, G.; Huang, H.; Xu, H.; Bo, S.; Qiu, L.; Zhen, Z.; Liu, X. *RSC Adv.* **2014**, *4*, 25532–25539.
- (9) Kwon, T.-H.; Armel, V.; Nattestad, A.; Macfarlane, D. R.; Bach, U.; Lind, S. J.; Gordon, K. C.; Tang, W.; Jones, D. J.; Holmes, A. B. *J. Org. Chem.* **2011**, *76*, 4088–4093.
- (10) Fix, A. G.; Chase, D. T.; Haley, M. M. *Top. Curr. Chem.* **2014**, *349*, in press (DOI: 10.1007/128_2012_376).
- (11) Chase, D. T.; Fix, A. G.; Rose, B. D.; Weber, C. D.; Nobusue, S.; Stockwell, C. E.; Zakharov, L. N.; Lonergan, M. C.; Haley, M. M. *Angew. Chem., Int. Ed. Engl.* **2011**, *50*, 11103–11106.
- (12) Chase, D. T.; Fix, A. G.; Kang, S. J.; Rose, B. D.; Weber, C. D.; Zhong, Y.; Zakharov, L. N.; Lonergan, M. C.; Nuckolls, C.; Haley, M. M. *J. Am. Chem. Soc.* **2012**, *134*, 10349–10352.
- (13) Miyata, Y.; Minari, T.; Nemoto, T.; Isoda, S.; Komatsu, K. *Org. Biomol. Chem.* **2007**, *5*, 2592–2598.
- (14) Nakagawa, T.; Kumaki, D.; Nishida, J.; Tokito, S.; Yamashita, Y. *Chem. Mater.* **2008**, *20*, 2615–2617.
- (15) Park, Y.; Lee, J. S.; Kim, B. J.; Kim, B.; Lee, J.; Kim, D. H.; Oh, S.; Cho, H.; Park, J. *Chem. Mater.* **2011**, *23*, 4038–4044.
- (16) Rose, B. D.; Chase, D. T.; Weber, C. D.; Zakharov, L. N.; Lonergan, M. C.; Haley, M. M. *Org. Lett.* **2011**, *13*, 2106–2109.
- (17) Zhou, Q.; Carroll, P. J.; Swager, T. M. *J. Org. Chem.* **1994**, *59*, 1294–1301.
- (18) Rose, B. D.; Santa Maria, P. J.; Fix, A. G.; Vonnegut, C. L.; Zakharov, L. N.; Parkin, S. R.; Haley, M. M. *Beil. J. Org. Chem.* **2014**, *10*, 2122–2130.
- (19) Thirion, D.; Rault-Berthelot, J.; Vignau, L.; Poriol, C. *Org. Lett.* **2011**, *13*, 4418–4421.
- (20) Duan, C.; Cai, W.; Zhong, C.; Li, Y.; Wang, X.; Huang, F.; Cao, Y. *J. Polym. Sci., Part A: Polym. Chem.* **2011**, *49*, 4406–4415.
- (21) (a) Marsden, J. A.; Miller, J. J.; Shirtcliff, L. D.; Haley, M. M. *J. Am. Chem. Soc.* **2005**, *127*, 2464–2476. (b) Arakawa, Y.; Nakajima, S.; Ishige, R.; Uchimura, M.; Kang, S.; Konishi, G.; Watanabe, J. *J. Mater. Chem.* **2012**, *22*, 8394–8398. (c) Wu, R.; Schumm, J. S.; Pearson, D. L.; Tour, J. M. *J. Org. Chem.* **1996**, *61*, 6906–6921. (d) Jo, S.-Y.; Hur, J.-A.; Kim, K.-H.; Lee, T.-W.; Shin, J.-C.; Hwang, K.-S.; Chin, B.-D.; Choi, D.-H. *Bull. Korean Chem. Soc.* **2012**, *33*, 3061–3070.
- (22) Cocherel, N.; Poriol, C.; Rault-Berthelot, J.; Barrière, F.; Audebrand, N.; Slawin, A. M. Z.; Vignau, L. *Chem.—Eur. J.* **2008**, *14*, 11328–11342.
- (23) (a) Pappenfus, T. M.; Seidenkranz, D. T.; Reiheimer, E. W. *Heterocycles* **2012**, *85*, 355–364. (b) Kanimozhi, C.; Balraju, P.; Sharma, G. D.; Patil, S. J. *Phys. Chem. B* **2010**, *114*, 3095–3103.